J MATER RES TECHNOL. 2019;8(3):3088–3096

Available online at www.sciencedirect.com

jmr&t Journal of Materials Research and Technology

www.jmrt.com.br

Original Article

Potentiodynamic polarization studies of Cefadroxil and Dicloxacillin drugs on the corrosion susceptibility of aluminium AA6063 in 0.5 M nitric acid

Ojo Sunday Isaac Fayomi[a,c,*], *I.Godwin Akande*[b], *Abimbola Popoola Idowu Popoola*[c], *Hlatswayo Molifi*[c]

[a] *Department of Mechanical Engineering, Covenant University, Ota, Ogun State, Nigeria*
[b] *Department of Mechanical Engineering, University of Ibadan, Ibadan, Oyo State, Nigeria*
[c] *Department of Chemical, Metallurgical and Materials Engineering, Tshwane University of Technology, Pretoria, South Africa*

ARTICLE INFO

Article history:
Received 3 October 2018
Accepted 13 December 2018
Available online 27 May 2019

Keywords:
Polarization
Aluminium
Interfaces
Passivation
Cefadroxil
Dicloxacillin

ABSTRACT

The inhibition effectiveness of Cefadroxil (C) and Dicloxacillin (D) drugs on aluminium in 0.5 M nitric acid solution have been holistically studied using potentiodynamic polarization techniques, weight loss measurements, computational studies and structural characterization. The structural characterizations were carried with the aid of scanning electron microscope equipped with energy dispersive spectrometer (SEM/EDS), optical microscope (OPM) and XRD. Potentiodynamic polarization test revealed the corrosion protectiveness and adsorbing ability of Cefadroxil and Dicloxacillin drugs on aluminium (Al). The mixed inhibitive characteristics of Cefadroxil and Dicloxacillin drugs were confirmed through the Tafel plot, which further established their predominant effect on the anodic reaction as a result of E_{corr} value shift to more positive sides. The combined effect of Cefadroxil and Dicloxacillin drugs reduced the exchange in current density and corrosion rate drastically from 484 μA/cm^2 to 199 μA/cm^2 and 0.4502 mm/year to 0.2152 mm/year respectively. 44.4% increase in microhardness was achieved and Inhibition efficiency of 58.9% was accomplished.

1. Introduction

Multi-industrial application and relevance of aluminium have necessitated the studies of its behaviour in a corrosive environment [1–4]. Research has shown that aluminium is the second most used metal for manufacturing and production in the world [5], exhibiting relatively good corrosion resistance compared to iron in different aggressive environment as a result of its ability to form a thin oxide film upon exposure [6,7]. Aluminium alloys are commonly employed in a marine environment where lighter density and superior mechanical

* *Corresponding author at: Tel. +2348036886783.*
E-mails: ojosundayfayomi3@gmail.com (O.S. Fayomi), aigodwin2015@gmail.com (I. Akande).
https://doi.org/10.1016/j.jmrt.2018.12.028

Table 1 – Chemical composition of aluminium alloy used (%w).

Fe	Mn	Cu	Si	Al
0.42	0.027	0.11	0.20	Balance

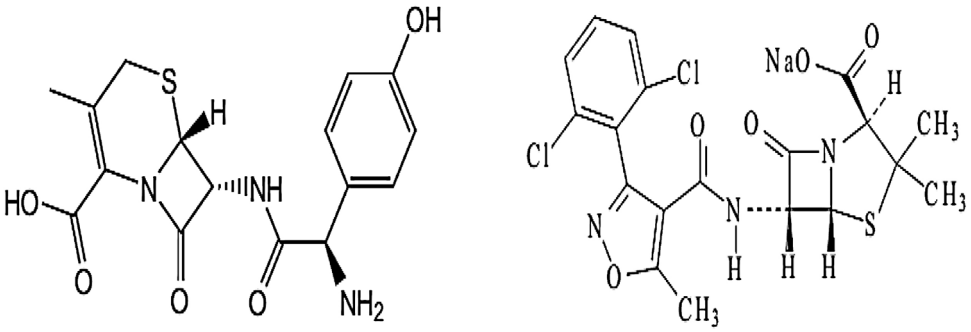

Fig. 1 – Molecular structure of Cefadroxil [29] and Dicloxacillin [30] respectively.

attributes are needed [8]. Marine corrosion takes place amidst parts of machine and piping that are exposed to contaminated water which might be acidic, alkaline or saline in nature. Susceptibility of components can be continuous or sporadic. Ships, pipelines, marine structures, are prevalent instances of systems that encounter marine degradation [9]. In recent years, wider usage of aluminium and its alloy in acidic and sodium chloride solution have exposed their vulnerability to attack by localized corrosion [10–14]. Hence, protection of aluminium from corrosion is imminent.

One of the recent corrosion protection measures involves doping metals with inhibitive drugs. Organic and inorganic compounds have provided protection against the corrosion of metal; however, some of them are poisonous, extremely expensive and difficult to synthesis from natural sources [15–18]. These reasons have evoked the attraction for inhibitive drugs in recent time, making it one of the most shot out methods through which metals are protected against corrosion [19–23]. Apart from the eco-friendly nature of inhibitive drugs, they are also been found to be cost effective, highly efficient and easy to synthesis [24,25]. The protective efficiency of drug inhibitors is a function of their absorbability on the surface of metals, thereby forming thin film of protective layer against attack by corrosive species in the environment [26]. Although, a lot of drugs, including the expired ones have infinitesimally provide corrosion resistance to metals in an aggressive environment [27,28]. In view of this, inhibitive capability of Cefadroxil and Dicloxacillin drugs on aluminium alloy was examined in 0.5 M nitric acid solution *via* potentiodynamic polarization techniques, mass loss measurements, computational studies and microstructural characterization.

2. Experimental procedures

2.1. Sample preparation

The chemical composition of type AA-6063 aluminium alloy obtained commercially from the aluminium rolling mill in Kempton Park, South Africa was analyzed in Table 1. Rectangular aluminium specimens were mechanically cut to size of (15 × 15 × 2) mm was used for the studies. The surfaces of the specimens were mechanically polished with different grades (400, 600 and 1200 μm) of emery papers, rinsed quickly with distilled water and allowed to dry naturally. 1 g of Cefadroxil and 1 g of Dicloxacillin sodium monohydrate white powders were obtained from Sigma-Aldrich in South Africa. They were prepared in volume concentrations 1.5 ml per 100 ml of 0.5 M HNO_3 acid. Cefadroxil and Dicloxacillin were diluted with distilled water to 10 ml concentrated solution. The molecular formula of Cefadroxil is $C_{16}H_{17}N_3O_5S$ and its molar mass is 363.39 g/mol. Molecular mass and molar mass of Dicloxacillin are $C_{19}H_{16}Cl_2N_3NaO_5S{\cdot}H_2O$ and 510.32 g/mol respectively. Molecular structure of Cefadroxil and Dicloxacillin are shown in Fig. 1.

2.2. Microstructural test of inhibited samples

The surface adhesion and texture of the of the inhibitor on the aluminium alloy were characterized using energy dispersive spectroscopy (EDS) attached to scanning electron microscope (SEM), OPM and XRD.

2.3. Microhardness testing

Vickers microhardness measurements were carried out on the inhibited and uninhibited specimens using an Emco test durascan microhardness tester equipped with Ecos workflow ultra-modern software. This can be obtained from Eq. (1). The indenting load of 100 g was applied during a testing period of 15 s, after which it was removed. The samples surface was indented randomly at five different positions and the average was recorded.

$$HV = 1.854\left(\frac{F}{d^2}\right) \quad (1)$$

F, load in kgf, and *d*, mean of two diagonal in mm.

2.4. *Linear polarization resistance*

The corrosive environment of 0.5 M HNO_3 was simulated in a beaker. Aluminium alloy coupon acting as the working electrode was welded to wire and mounted on resin. Graphite rod was used as the counter electrode immersed in solution and silver chloride electrode (SCE) acting as reference electrode was placed on sample surface. Autolab PGSTAT 101 Metrohm potentiostat/galvanostat with NOVA software of version 2.1.2 was used with linear polarization (LR) resistance and the current was set to 10 mA (max) and 10 nA (min). LSV staircase parameter start potential of −1.5 V, step potential 0.001 m/s and stop potential of 1.5 V set for 60 min. This was repeated for about five times for the aluminium in 0.5 M HNO_3 simulated solution without inhibitors and with 1.5 ml Cefadroxil, 1.5 ml Dicloxacillin, 1.5 ml Cefadroxil + 1.5 ml Dicloxacillin inhibitors so as to check for reproducibility. Applied potential *vs*. current density were plotted and on extrapolation of linear portion, the corrosion potential and corrosion current were obtained. In anodic and cathodic plot, the slope of the linear portion gives Tafel constants 'b_a' and 'b_c' respectively. According to

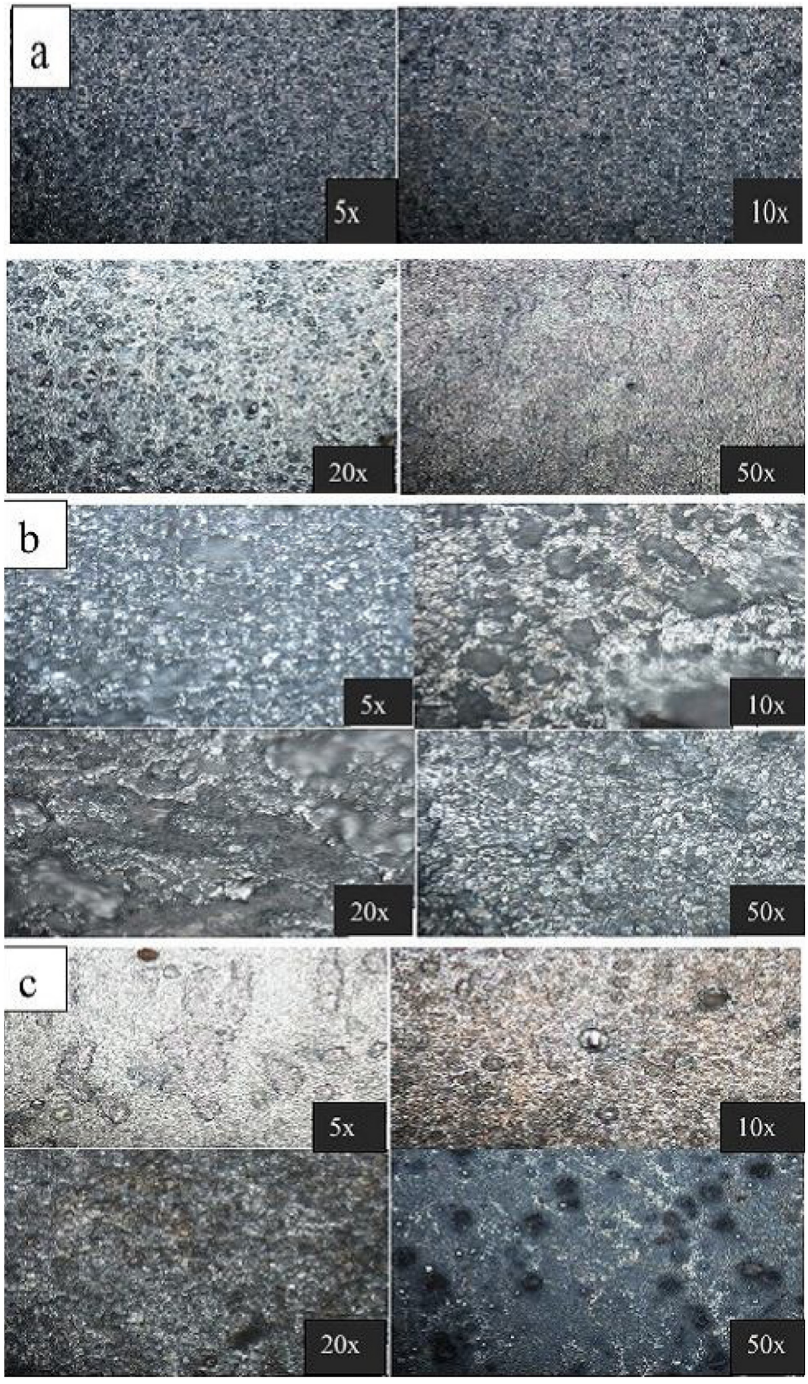

Fig. 2 – Optical micrographs of Al alloy with (a) 1.5 Cefadroxil, (b) 1.5 Dicloxacillin and (c) 1.5 Cefadroxil + 1.5 Dicloxacillin inhibitor after potentiodynamic experiment.

Stern–Geary equation, shown in Eq. (2), the steps of the linear polarization plot are substituted to get corrosion current.

$$I_{corr} = \frac{(b_a \times b_c)}{2.303(b_a + b_c) \times R_p} \quad (2)$$

where PR is the polarization resistance.

Inhibition efficiencies (IE) were calculated using Eq. (3)

$$IE(\%) = \frac{(j_{corr} - j_{ocorr})}{j_{corr}} \times 100 \quad (3)$$

j_{ocorr}, corrosion current without inhibitor and j_{corr}, corrosion current with inhibitor.

2.5. *Weight loss experiment*

Aluminium coupon samples of dimension $(15 \times 15 \times 2)$ mm were prepared, drilled at one end and polished with abrasive paper, rinsed with distilled water and allowed to dry. The pre-cleaned and weighed samples were suspended in beakers using glass hooks and rods containing the test solutions of different concentrations of 0.1; 0.3; 0.5 and 1.0 ml. Tests were conducted under total immersion conditions in 25 ml of the solution. Immersion time was varied from 1 to 21 days (504 h). The samples were retrieved from test solutions after every 72 h, appropriately cleaned, dried and reweighed. The weight loss was taken to be the difference between the weight of the samples at a given time and its initial weight.

The corrosion rate (R) values are obtained by using Eq. (4)

$$R = \frac{87.6W}{DAT} \quad (4)$$

where W is the weight loss in milligrams, D, the density in g/cm^2, A, the area in cm^2, and T, is the time of exposure in hours.

The %IE was calculated from the relationship:

$$\%\,(IE)\,\text{inhibition efficiency} = (W_1 - W_2)/W_1 \quad (5)$$

where W_1 and W_2 are the weight loss in the absence and presence of inhibitors. The %IE was calculated for all the inhibitors every 72 h during the course of the experiment, while the surface coverage is calculated from the relationship:

$$\theta = \left[1 - \frac{W_1}{W_2}\right] \quad (6)$$

θ is the amount of substance adsorbed per gram (or kg).

3. Results and discussion

3.1. *Surface morphology and structural analysis of the inhibited samples*

The optical micrographs in Fig. 2 affirmed the uniform dispersion of inhibitive drug particles synergistically embedded on the surface of aluminium alloy. Particles embedded on the alloy surface promote increase number of nucleation site thereby preventing crystal growth which eventually resulted in small-sized grains [31]. The refined microstructure could be attributed to the natural ability of Cefadroxil and Dicloxacillin drugs to adhere uniformly to metal surfaces. It is worthy of note that the uniform distribution and small micro link around major lattice generates adorable and compatible grains in the structure. Fig. 2a revealed that the surface of 1.5 Cefadroxil inhibited Al alloy appeared the smoothest exhibiting the finest morphology while 1.5 Dicloxacillin inhibited Al alloy in Fig. 2b is the roughest with the coarsest morphology.

The optical micrograph in Fig. 3 indicates different magnification of 1.5 Cefadroxil + 1.5 Dicloxacillin inhibited sample after weight loss experiment. Regular shaped, uniformly dispersed, darker and shiny particles of the inhibitive drugs were observed to have adsorbed on the surface of the metal. The darkened nature of the inhibited surface could be attributed to longer period of time Al alloy spent in the corrosive medium compared to the time spent during the potentiodynamic experiment.

SEM/EDS micrographs of Al samples after corrosion test and weight loss experiment are shown in Fig. 4a and b respectively. SEM images of the samples shows that the pitting evolution at the interface was not visible after the corrosion and weight loss experiment. Good surface topography and morphological were observed due to the inability

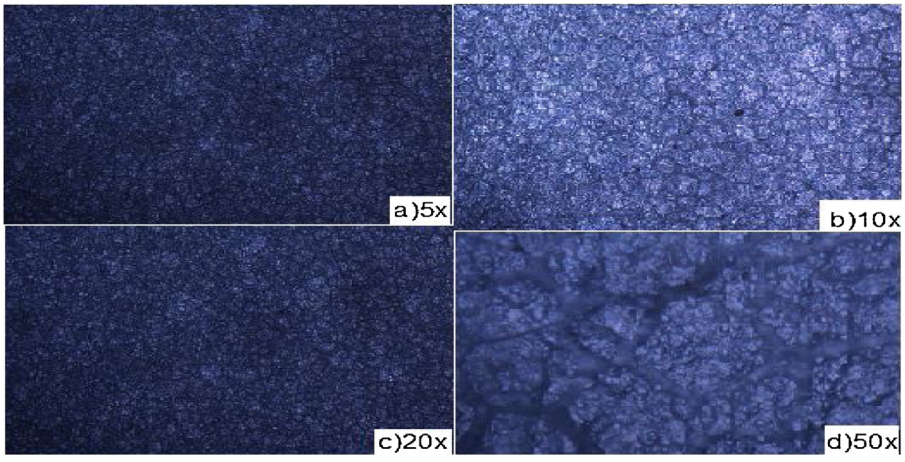

Fig. 3 – Optical micrographs of Al alloy with 1.5 Cefadroxil + 1.5 Dicloxacillin inhibitor after weight loss experiment.

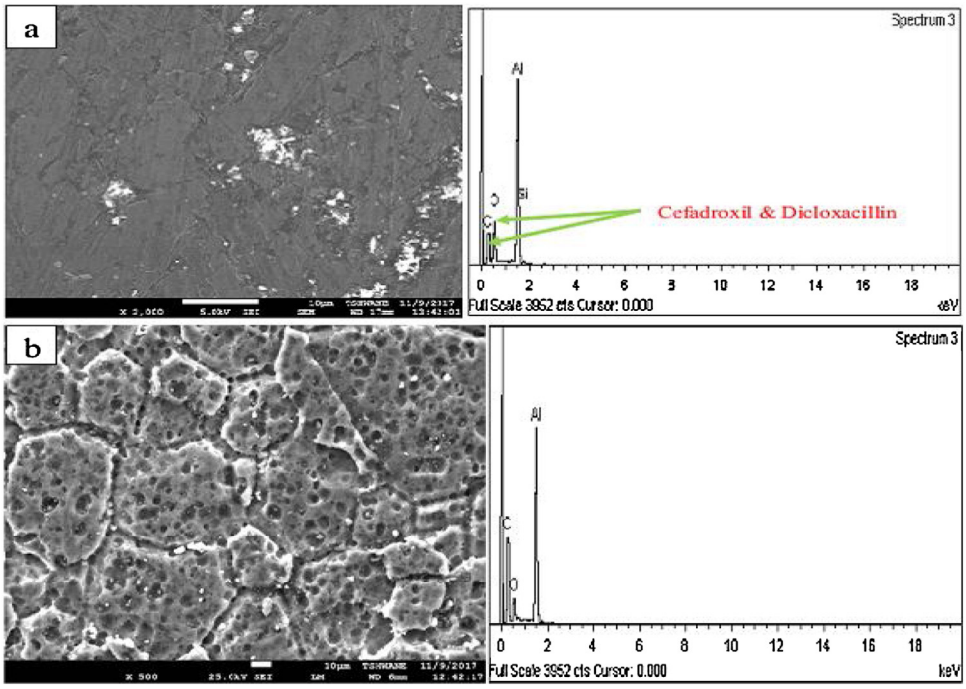

Fig. 4 – SEM/EDS micrographs of Al alloy with 1.5 Cefadroxil + 1.5 Dicloxacillin inhibitor after (a) corrosion test and (b) weight loss experiment.

of corrosive ion to ingress the inhibited surface. Although the surface of the sample used for the weight loss experiment as shown in Fig. 4b was observed to be rougher, but the metal surface was better covered than that Fig. 4a. The natural adsorbing effect of the inhibitors minimizes the redox chemical reactions that would have caused the discharge of valence electrons by the nitride ion and diffusion of Al^{3+} cations in the nitride solution. The SEM images in

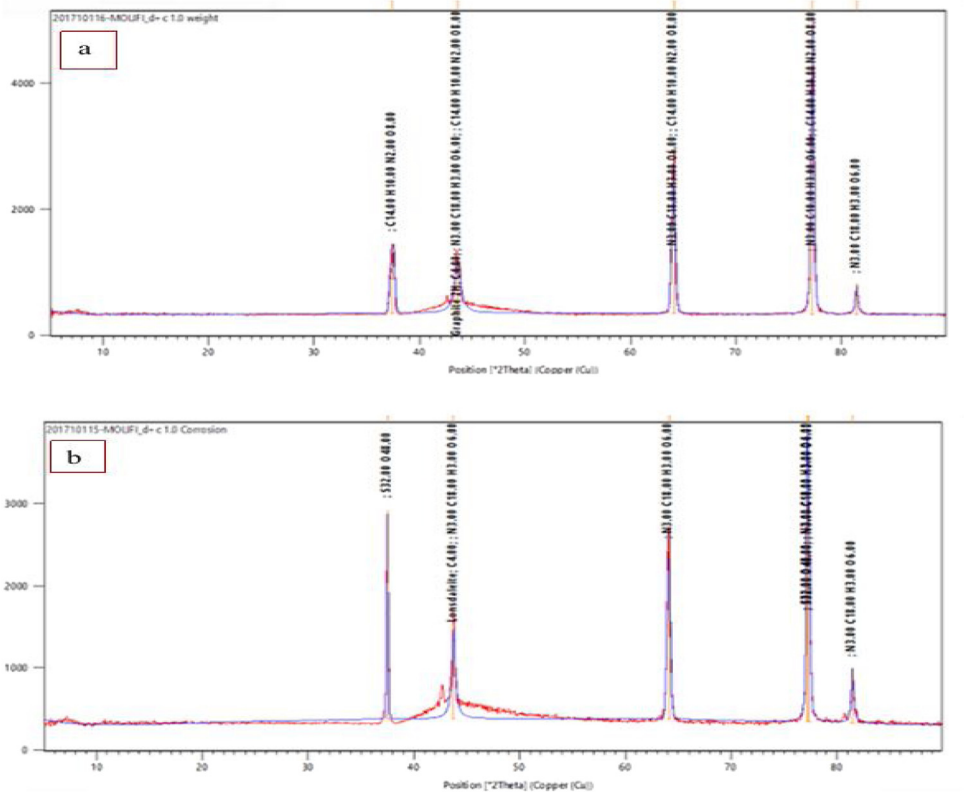

Fig. 5 – XRD of Al alloy with 1.5 Cefadroxil + 1.5 Dicloxacillin after (a) weight loss, (b) potentiodynamic experiment.

Table 2 – Polarization data for inhibited and uninhibited aluminium in acid media.

Samples	E_{corr} obs (V)	j_{corr} (μA/cm^2)	b_a (V/dec)	b_c (V/dec)	CR (mm/year)	PR (Ω)
Control	−0.6760	484	0.4251	0.6443	0.4502	230.0
1.5 Dicloxacillin	−0.2554	342	0.1408	0.1941	0.3710	103.60
1.5 Cefadroxil	−0.3702	287	0.2648	0.4564	0.2926	253.83
1.5 Dicloxacillin + 1.5 Cefadroxil	−0.2920	199	0.3479	1.0459	0.2152	570.96

accordance with the work of author in reference [32] reveal mild scars on the surface indicating the adsorption characteristics of the inhibitive drugs on the aluminium interface, through physico-chemical reaction. It is significant to note that the EDS image in Fig. 4a and b confirms the presence the presence of Cefadroxil and Dicloxacillin, establishing the natural adhesive ability and dispersive strength [33] of the antibiotic inhibitive drugs.

Fig. 5 shows the intermediate dispatched inhibiting phases observed from XRD patterns for the Cefadroxil and Dicloxacillin inhibited aluminium alloy. From the pattern, visible build-up phases of strong intermetallic precipitate leads to fine grain structure. Generation of intermetallic phases of Cefadroxil and Dicloxacillin present was ascertained by the intensities and degrees of diffractive angle patterns. The main peaks found are Al and Al-C-D at 2θ Braga angle intensity of = (37.50°, 43.52°, 64.30°, 77.50°, 81.50°) for the XRD in Fig. 5a. Fig. 5b has 2θ Braga angle intensity of = (37.50°, 44.10°, 64.30°, 77.50°, 81.50°) which is similar to the values in Fig. 5a. In comparison with literature studies, the height of any peak is considered an indication of quantity of phase deposit [34]. From observation, the inhibitive effect of Cefadroxil and Dicloxacillin result in new orientation of the metal particle precipitate contributing to the strong character and adsorbing tendency of individual inhibitor. It should be noted that the presence of Cefadroxil and Dicloxacillin drug inhibitors led to the visible interfacial formation depicted by the red like phases on the alloy surface which are more visible in Fig. 5b.

3.2. *Linear potentiodynamic polarization*

Potentiodynamic data of aluminium in 0.5 M HNO_3 in the absence and presence of Dicloxacillin and Cefadroxil drugs are shown in Table 2. The resulting polarization curves are shown in Fig. 6. The potentiodynamic study revealed that the inhibitors reduced the anodic and cathodic reaction,

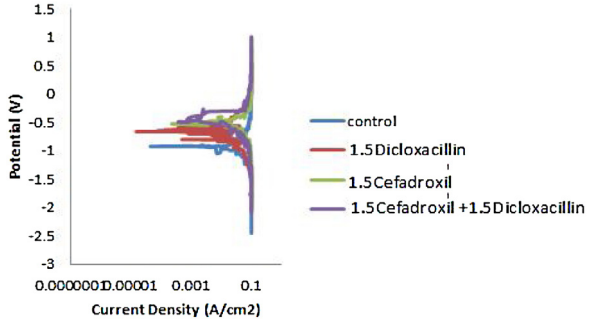

Fig. 6 – Cathodic and anodic polarization scans for aluminium substrate with and without inhibitive drugs in 0.5 M HNO_3.

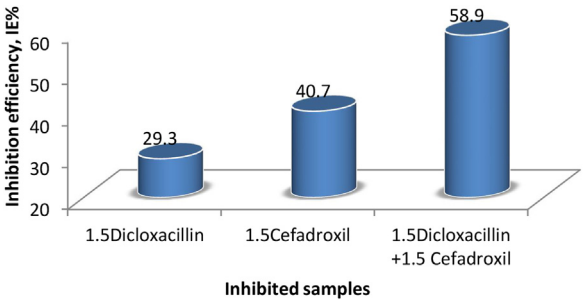

Fig. 7 – Inhibitor efficiency of inhibited samples.

thereby minimizing the corrosion current density (j_{corr}). Although, these inhibitors are mixed-type but predominantly anodic. The anodic inhibitive characteristics of Cefadroxil and Dicloxacillin influenced the shift in the values of corrosion potential (E_{corr}) to more positive side relative to the uninhibited samples indicating that the inhibitors affected the anodic reaction more than the cathodic reaction, adsorbing its molecules on the surface of the aluminium and consequentially incapacitating the mobility of the nitride ion (N^{3-}) to the active site to the metal [35,36].

3.3. *Inhibition efficiency of Cefadroxil and Dicloxacillin*

Fig. 7 shows the inhibition efficiency of the used inhibitors. It can be seen that the synergistic combination of Cefadroxil and Dicloxacillin exhibit the best corrosion inhibition efficiency. However, application of Cefadroxil and Dicloxacillin individually inhibits aluminium by 40.7% and 29.3% respectively. The inhibition efficiency of these drugs is as a result of the interaction and reduction of complex activities on the coverage site [37].

3.4. *Influence of Cefadroxil and Dicloxacillin on corrosion rate of aluminium*

The values of corrosion rates (CR) represented in Fig. 8 were found to reduce in the presence of the added inhibitors.

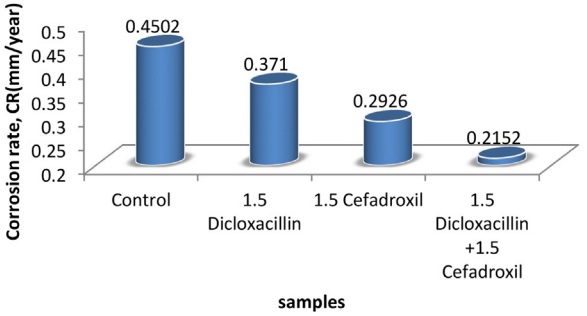

Fig. 8 – Corrosion rate of the aluminium samples.

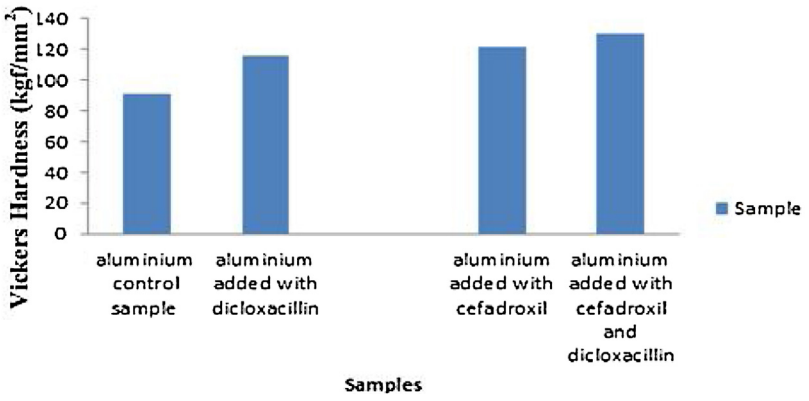

Fig. 9 – Microhardness comparison of uninhibited and inhibited aluminium in linear polarization experiment.

The minimum corrosion rate was found with the 1.5 Cefadroxil + 1.5 Dicloxacillin inhibited sample. The reduction in the rate of corrosion could be as a result of the synergy between the molecules of the two drugs. The synergetic effect of these inhibitive drugs invigorates the binding energy between them, leading to their continuous adsorption on the surface of the metal. Cefadroxil and Dicloxacillin like most antibiotics and their decomposition products possess electron donor groups that can bind naturally occurring metal ions, there by forming complexes with metal ions [38].

3.5. *Microhardness behaviour of inhibited and uninhibited samples*

The microhardness results obtained for Cefadroxil and Dicloxacillin inhibited and uninhibited samples are represented in Fig. 9. Comparison of the hardness results revealed that 1.5 Cefadroxil + 1.5 Dicloxacillin inhibited aluminium possess 130 kgf/mm^2, which is the highest value of hardness in the series. This value of hardness depicts 44.4% increase in hardness compared to the uninhibited aluminium with the hardness value of 90 kgf/mm^2. The individual usage of the drugs notably improved the microhardness of aluminium as shown in Fig. 9. Improvement in microhardness could be attributed to the formation of intermetallic adhesives and synergetic mechanism by the inhibitive drugs on the substrate samples.

3.6. *Weight loss measurement*

Results obtained from weight loss measurements are shown Fig. 10. It can be seen that introduction of the inhibitive drugs to the corrosive medium was observed to have had notable effect on the rate of weight loss. Combined synergetic effect of Cefadroxil and Dicloxacillin on aluminium alloy impedes the weight loss better than the individual application as shown in Fig. 10. The minimal weight loss is as a result of the ability of Cefadroxil and Dicloxacillin to form strong adhesive layer on the metal surface like some other antibiotic. This result is in good agreement with corrosion characteristics observed by author in references [39,40].

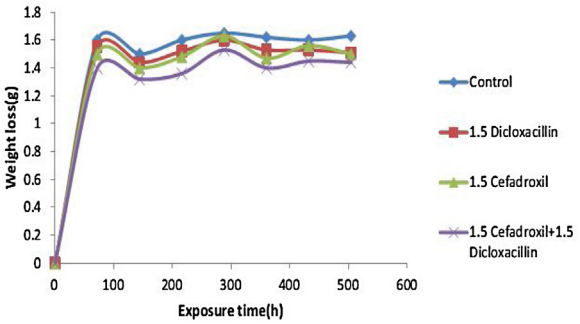

Fig. 10 – Variation of weight loss by the inhibited and uninhibited samples.

4. Conclusions

In summary, this work reported the effect of Cefadroxil and Dicloxacillin inhibitive drugs applied synergistically on the surface of aluminium alloy. It was confirmed that these inhibitors had significant impact on the structural build-up of the base metal resulting to the reduction of current density and corrosion rate. The inhibited samples show uniform growth, flawless crystals and improved inhibition efficiencies. There is no doubt that the formation of intermetallic adhesives and synergetic mechanism by the inhibitive drugs on the metal surface was responsible for the improvement of microhardness.

Conflicts of interest

The authors declare no conflicts of interest.

Acknowledgements

The authors acknowledged the research publication support received from Covenant University Centre for Research and Innovation Development (CUCRID) and the opportunity offered by Surface Engineering Research Centre, Tshwane University of Technology Pretoria, South Africa to carry out this experiment.

REFERENCES

[1] Oguzie EE. Corrosion inhibition of aluminium in acidic and alkaline media by *Sansevieria trifasciata* extract. Corros Sci 2007;49(3):1527–39.

[2] Li X, Deng S, Fu H. Inhibition by tetradecylpyridinium bromide of the corrosion of aluminium in hydrochloric acid solution. Corros Sci 2011;53(4):1529–36.

[3] Oguzie EE, Okolue BN, Ebenso EE, Onuoha GN, Onuchukwu AI. Evaluation of the inhibitory effect of methylene blue dye on the corrosion of aluminium in hydrochloric acid. Mater Chem Phys 2004;87(2–3):394–401.

[4] Fayomi OSI, Abdulwahab M, Popoola AP, Asuke F. Corrosion resistance of AA6063-type Al-Mg-Si alloy by silicon carbide in sodium chloride solution for marine application. J Mar Sci Appl 2015;14(4):459–62.

[5] Prabhu D, Rao P. *Coriandrum sativum* L.—a novel green inhibitor for the corrosion inhibition of aluminium in 1.0 M phosphoric acid solution. J Environ Chem Eng 2013;1(4):676–83.

[6] Krishnaveni K, Ravichandran J. Effect of aqueous extract of leaves of *Morinda tinctoria* on corrosion inhibition of aluminium surface in HCl medium. Trans Nonferrous Met Soc China 2014;24(8):2704–12.

[7] Fayomi OSI, Abdulwahab M. Degradation behaviour of aluminium in 2 M HCl/HNO_3 in the presence of arachis hypogeae natural oil. Int J Electrochem Sci 2012;7:5817–27.

[8] Ezuber H, El-Houd A, El-Shawesh F. A study on the corrosion behavior of aluminum alloys in seawater. Mater Des 2008;29(4):801–5.

[9] Rosliza R, Nik WW. Improvement of corrosion resistance of AA6061 alloy by tapioca starch in seawater. Curr Appl Phys 2010;10(1):221–9.

[10] Halambek J, Berković K, Vorkapić-Furač J. *Laurus nobilis* L. oil as green corrosion inhibitor for aluminium and AA5754 aluminium alloy in 3% NaCl solution. Mater Chem Phys 2013;137(3):788–95.

[11] Moore KL, Sykes JM, Hogg SC, Grant PS. Pitting corrosion of spray formed Al–Li–Mg alloys. Corros Sci 2008;50(11):3221–6.

[12] Sherif ES. Corrosion and corrosion inhibition of aluminum in Arabian Gulf seawater and sodium chloride solutions by 3-amino-5-mercapto-1,2,4-triazole. Int J Electrochem Sci 2011;6(5):1479–92.

[13] Pyun SI, Na KH, Lee WJ, Park JJ. Effects of sulfate and nitrate ion additives on pit growth of pure aluminum in 0.1 M sodium chloride solution. Corrosion 2000;56(10):1015–21.

[14] Blücher DB, Svensson JE, Johansson LG. The NaCl-induced atmospheric corrosion of aluminum the influence of carbon dioxide and temperature. J Electrochem Soc 2003;150(3):93–8.

[15] Ofoegbu SU, Ofoegbu PU. Corrosion inhibition of mild steel in 0.1 M hydrochloric acid media by chloroquine diphosphate. ARPN J Eng Appl Sci 2012;7(3):272–6.

[16] Kumar H, Karthikeyan S. Inhibition of mild steel corrosion in hydrochloric acid solution by cloxacillin drug. J Mater Environ Sci 2012;3(5):925–34.

[17] Edison TN, Atchudan R, Pugazhendhi A, Lee YR, Sethuraman MG. Corrosion inhibition performance of spermidine on mild steel in acid media. J Mol Liq 2018;264:483–9.

[18] Winkler DA, Breedon M, White P, Hughes AE, Sapper ED, Cole I. Using high throughput experimental data and in silicon models to discover alternatives to toxic chromate corrosion inhibitors. Corros Sci 2016;106:229–35.

[19] Gece G. Drugs: a review of promising novel corrosion inhibitors. Corros Sci 2011;53(12):3873–98.

[20] Shukla SK, Quraishi MA. Cefalexin drug: a new and efficient corrosion inhibitor for mild steel in hydrochloric acid solution. Mater Chem Phys 2010;120(1):142–57.

[21] Obot IB, Obi-Egbedi NO, Umoren SA. Antifungal drugs as corrosion inhibitors for aluminium in 0.1 M HCl. Corros Sci 2009;51(8):1868–75.

[22] Shukla SK, Singh AK, Ahamad I, Quraishi MA. Streptomycin: A commercially available drug as corrosion inhibitor for mild steel in hydrochloric acid solution. Mater Lett 2009;63(9–10):819–22.

[23] Fouda AS, Mostafa HA, El-Abbasy HM. Antibacterial drugs as inhibitors for the corrosion of stainless steel type 304 in HCl solution. J Appl Electrochem 2010;40(1):163–73.

[24] Raja PB, Qureshi AK, Rahim AA, Osman H, Awang K. Neolamarckia cadamba alkaloids as eco-friendly corrosion inhibitors for mild steel in 1 M HCl media. Corros Sci 2013;69:292–301.

[25] Verma C, Ebenso EE, Bahadur I, Obot IB, Quraishi MA. 5-(Phenylthio)-3H-pyrrole-4-carbonitriles as effective corrosion inhibitors for mild steel in 1 M HCl: experimental and theoretical investigation. J Mol Liq 2015;212:209–18.

[26] Umoren SA, Obot IB, Ebenso EE, Okafor PC, Ogbobe O, Oguzie EE. Gum Arabic as a potential corrosion inhibitor for aluminium in alkaline medium and its adsorption characteristics. Anti-Corros Methods Mater 2006;53(5):277–82.

[27] Nazeer AA, El-Abbasy HM, Fouda AS. Antibacterial drugs as environmentally-friendly corrosion inhibitors for carbon steel in acid medium. Res Chem Intermed 2013;39(3):921–39.

[28] Singh P, Chauhan DS, Srivastava K, Srivastava V, Quraishi MA. Expired atorvastatin drug as corrosion inhibitor for mild steel in hydrochloric acid solution. Int J Ind Chem 2017;8(4):363–72.

[29] Almasri I, Ramadan M, Khayal G. Spectrophotometric determination of Cefadroxil in bulk and dosage forms using 2,4-dinitrophenylhydrazine. J Al Azhar Univ-Gaza (Nat Sci) 2015;17:129–46.

[30] Alderete O, González-Esquivel DF, Del Rivero LM, Torres NC. Liquid chromatographic assay for Dicloxacillin in plasma. J Chromatogr B 2004;805(2):353–6.

[31] Anawe PA, Raji O, Fayomi OS, Efeovbohkan VE. Influence of composite nano coating on ternary sulphate co-deposition: corrosion and surface characterization. Procedia Manuf 2017;7:556–61.

[32] Fayomi OSI, Bamgboye OA, Durodola BM, Inam WA, Daniyan AA. Adsorption and corrosion inhibition properties of floxapen compound on the electrochemical characteristics of type-A5-series aluminium in sodium chloride solution. Int J Microstruct Mater Prop 2017;12(5–6):391–401.

[33] Fayomi OSI, Atayero AA, Mubiaye P, Akande IG, Adewuyi PA, Fajobi MA, et al. Mechanical and opto-electrical response of embedded smart composite coating produced via electrodeposition technique for embedded system in defence application. J Alloys Compd 2019;773:305–13.

[34] Fayomi OSI, Monyai T. Wear stress mitigation and structural characteristics of highly performing zinc-based induced ZrO_2/ZrN composite alloy coating on mild steel. Int J Adv Manuf Technol 2018;96(5–8):1813–21.

[35] Dohare P, Chauhan DS, Hammouti B, Quraishi MA. Experimental and DFT investigation on the corrosion inhibition behavior of expired drug lumerax on mild steel in hydrochloric acid anal. Bioanal Electrochem 2017;9:762.

[36] Fouda AS, Mahmoud WM, Mageed HA. Evaluation of an expired nontoxic amlodipine besylate drug as a corrosion inhibitor for low-carbon steel in hydrochloric acid solutions. J Bio Tribo-Corros 2016;2(2):7.

[37] Fayomi OSI. The inhibitory effect and adsorption mechanism of roasted *Elaeis guineensis* as green inhibitor on the corrosion process of extruded AA6063 Al-Mg-Si alloy in simulated solution. Silicon 2014;6(2):137–43.

[38] Muthu K, Gunasekaran K, Kala A, Govindasamy P, Rajesh P, Moorthi PP. Spectroscopic (FT-IR, FT-Raman & UV-Vis) and density functional theory studies of Cefadroxil. Int. J. Curr. Microbiol. Appl. Sci 2015;4(11):211–25.
[39] Popoola API, Fayomi OSI, Abdulwahab M. Degradation behaviour of aluminium in 2 M HCl/HNO_3 in the presence of arachis hypogeae natural oil. Int J Electrochem Sci 2012;7:5817–27.
[40] Attar T, Larabi L, Harek Y. The inhibition effect of potassium iodide on the corrosion of pure iron in sulphuric acid. Adv Chem 2014;2014.